ELSEVIER

Thermochimica Acta 290 (1997) 191–197

thermochimica acta

Influence of molecular weight on the thermal decomposition of hydroxyl terminated polybutadiene

Sreelatha S. Panicker, K.N. Ninan*

Propellant and Special Chemicals Group, Vikram Sarabhai Space Centre, Thiruvananthapuram, 695022, India

Received 15 April 1996; revised 7 August 1996; accepted 1 September 1996

Abstract

Thermogravimetric analysis of hydroxyl terminated polybutadiene (HTPB) and its fractions of different molecular weights separated by preparative GPC shows two major stages of weight loss of different nature in a nitrogen atmosphere. The first stage is primarily depolymerisation, cyclisation and crosslinking of molecules and the second stage is mainly the decomposition of the residue from the first stage. The kinetic parameters, viz. activation energy E and pre-exponential factor A using four different non-isothermal integral equations show a systematic increase with increase in molecular weight for the first stage, whereas for the second stage, the effect of molecular weight on E and A values is not prominent. The increase in E and A values for the first stage is attributed to the formation of greater number of cyclised and crosslinked products from molecules of higher dimensions. Quantitative correlations between the kinetic constants and the molecular weight parameters were derived for the first stage as a quadratic curve following the equation: E or $\ln A = K_1 - K_2/M$ (where K_1 and K_2 are empirical constants whose values are different for the different molecular weight averages, viz. M_n, M_w and M_z and for the different equations). © 1997 Elsevier Science B.V.

Keywords: GPC molecular weight; HTPB; Kinetic parameters; Solid propellant binder; Thermal decomposition

1. Introduction

Hydroxyl terminated polybutadiene (HTPB) is a prepolymer used as the binder matrix in composite solid rocket propellants and is considered as the workhorse in the world scenario today. This is because of the high ballistic and mechanical properties imparted by the resin matrix. The combustion of solid propellants proceeds through a series of complex physicochemical processes. Therefore, a knowledge of the kinetics and mechanism of the thermal decomposition behaviour of the binder is essential for establishing appropriate models for the solid propellant combustion [1]. The ballistic performance of composite propellants based on polymeric binders like HTPB is dependent on the thermal decomposition of the binder [2,3] and the temperature of the burning surface of the corresponding solid propellant.

Thermal properties of HTPB have been studied by several workers [3–11]. Pyrolysis studies of polymeric binders with emphasis on functionally terminated polybutadienes have been reviewed by Beck [4]. Ninan et al. [5] have reported a thermogravimetric study on the thermal decomposition kinetics of carboxyl terminated polybutadiene (CTPB) and HTPB

*Corresponding author. Tel.: 56 2096 & 56 3689; fax: 0471 461795.

PII S0040-6031(96)03083-3

prepared by different routes. The effect of procedural factors such as sample mass and heating rate on the kinetic parameters (energy of activation E and pre-exponential factor A) was reported in the study. In a subsequent paper Ninan et al. [6] have studied the effect of molecular weight on the overall decomposition kinetics of HTPB. Ninan et al. [7] have also reported the effect of atmosphere on the thermal decomposition of HTPB. The studies by Tingfa [8] and Deyuan [9] have shown that the decomposition of HTPB involves two distinct stages of mass loss and they have suggested the structure of the products formed in both the stages with the help of gas chromatograph and mass spectrometer. Tingfa [8,10] studied the kinetics of decomposition of HTPB under different experimental conditions, viz. sample mass and heating rate, using a TG–DTG–DSC simultaneous system interfaced with a gas chromatograph and has shown the importance of kinetic data of HTPB binder in solid propellant combustion.

In the present work, it is attempted to evaluate the relative influence of the molecular weight distribution on the kinetics of the two stages of thermal decomposition of HTPB by thermogravimetry. Samples having different molecular weights are obtained by fractionating a particular batch of HTPB according to its molecular weight.

2. Experimental

2.1. Materials

HTPB–NOCIL, Bombay: made by the free-radical polymerisation of butadiene gas using H_2O_2 as initiator, using a process developed by Vikram Sarabhai Space Centre [12].

Solvents: Toluene and tetrahydrofuran (THF) of HPLC grade.

2.2. Fractionation of HTPB

HTPB was separated into five fractions of different molecular weights on a preparative gel permeation chromatograph, Waters Delta Prep equipped with R 401 differential refractive index (DRI) and R 481 UV absorbance detectors. Styragel columns (122 cm × 20 mm i.d.) of pore sizes 10^4 Å, 10^3 Å and 500 Å were used with toluene as the solvent at a flow rate of 15 ml min^{-1}. Since the preparative GPC could efficiently fractionate only about 1 g per run, repeated runs were made to collect sufficient quantity of each fraction. For each run 10 ml of a 10% solution in THF was used. Solvent was removed from the fractions by distillation and dried at reduced pressure.

2.3. Molecular weight and molecular weight distribution (MWD)

Molecular weight averages and molecular weight distribution of HTPB and fractions were determined using a Waters Associates GPC (Model 244). Four micro Styragel columns of pore sizes 10^4 Å, 10^3 Å, 500 Å and 100 Å were employed. Tetrahydrofuran was used as the solvent at a flow rate of 2 ml min^{-1}. Dual detector system of differential refractive index (DRI) and UV detectors was used. For each analysis, 100 µl of 1% solution was used. The column set was calibrated using Universal calibration [13].

2.4. Thermal studies

Thermal decomposition of the samples was studied using a Dupont-model 2000 thermal analyst in conjunction with 951 thermogravimetric analyser. The analyses were conducted in pure and dry nitrogen at a flow rate of 50 cm^3 min^{-1} and a heating rate of 10°C min^{-1}.

2.5. Calculation of kinetic parameters

Of the numerous equations available, the following four integral equations are used in this work for determining the kinetic parameters, viz. energy of activation E and pre-exponential factor A.

(1) Coats–Redfern (CR) equation [14]:

$$\ln\frac{g(\alpha)}{T^2} = \ln\frac{AR}{\phi E}\left(1 - \frac{2RT}{E}\right) - \frac{E}{RT}$$

(2) MacCallum–Tanner (MT) equation [15]:

$$\log g(\alpha) = \log\frac{AE}{\phi R} - 0.483E^{0.435} - \frac{(0.449 + 0.217E) \times 10^3}{T}$$

(3) Horowitz–Metzger (HM) equation [16]:

$$\ln g(\alpha) = \ln\frac{ART_s^2}{\phi E} - \frac{E}{RT_s} + \frac{E\Theta}{RT_s^2}$$

(4) Madhusudanan–Krishnan–Ninan (MKN) equation [17]:

$$\ln\frac{g(\alpha)}{T^{1.9215}} = \ln\frac{AE}{\phi R} + 3.7721 - 1.9215\ln E - \frac{0.12039E}{T},$$

where $g(\alpha) = \frac{1-(1-\alpha)^{1-n}}{1-n}$ for all values of n except $n=1$ for which $g(\alpha)=-\ln(1-\alpha)$

α	the fraction decomposed
n	order parameter
T	temperature (K)
R	universal gas constant
T_s	DTG peak temperature
ϕ	heating rate
Θ	$T-T_s$

The order parameters for the first and second stages of decomposition were obtained using the Coats–Redfern equation by an iteration method. Using a computer, linear plots of $\ln(g(\alpha)/T^2)$ vs. $1/T$ were drawn for different values of 'n' ranging from 0 to 2, in increments of 0.1. The value of 'n' which gave the best fit with correlation coefficient nearest to unity was chosen as the order parameter for each stage of decomposition. This value of 'n' is substituted in the four kinetic equations mentioned above. The left-hand side of the kinetic equations were plotted against $1/T$ except for the Horowitz–Metzger equation, for which left-hand side was plotted against Θ. The values of E and A were obtained from the slope and intercept of the straight lines, respectively.

The goodness of the curve fit was tested with appropriate statistical analysis and reliability tests. The linear curves were drawn by the method of least squares and the corresponding correlation coefficients, 'r' were calculated. The reliability of the non-linear curve fits was established by the F-test [18]. All the computational work was done on a PC/XT using a BASIC programme.

3. Results and discussion

3.1. Molecular weight

The schedule of fractionation by preparative GPC was aimed at obtaining roughly equal amounts of each fraction. The MWD curves of the fractions obtained are shown in Fig. 1. The weight percent of each fraction and the corresponding molecular weight averages, viz. number-average molecular weight (M_n), weight-average molecular weight (M_w), Z-average molecular weight (M_z) and polydispersity (d) are presented in Table 1 which shows a steady decrease in molecular weight with fraction number as expected in a GPC fractionation. The efficiency of fractionation is seen from the narrow polydispersity (M_w/M_n) values of the fractions (1.3 to 1.6 against 3.4 for unfractionated HTPB).

3.2. Thermal decomposition study

A typical TG/DTG curve of HTPB is given in Fig. 2 which shows two stages of mass loss. The first stage of reaction is in the range of 300 to 410°C and the second stage in the range of 410 to 510°C. The initial tem-

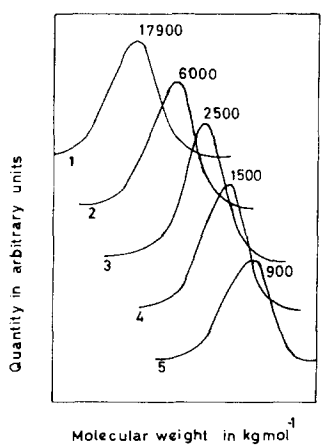

Fig. 1. GPC molecular weight distribution curves of HTPB fractions.

Table 1
GPC analysis of HTPB and fractions

Sample	Weight (%)	M_n	M_w	M_z	d
Fr. No. 1	17	14980	22400	33200	1.5
Fr. No. 2	19	5690	7930	11030	1.4
Fr. No. 3	30	2360	3150	4310	1.3
Fr. No. 4	19	1260	1690	2250	1.3
Fr. No. 5	15	660	1080	1880	1.6
HTPB	—	2550	8670	28670	3.4

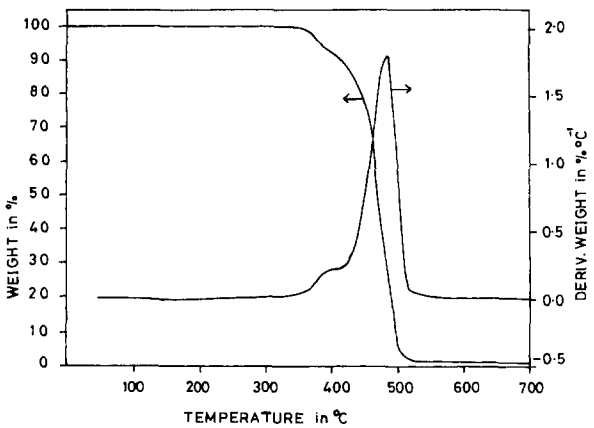

Fig. 2. TG/DTG curve of HTPB.

perature (T_i), final temperature (T_f), and peak temperature (T_s) for the first and second stages of decomposition, together with the mass loss data are given in Table 2. The mechanism of decomposition of HTPB is similar to that of polybutadiene [8,9,19]. The first stage is primarily depolymerisation, cyclisation and crosslinking, accompanied by partial decomposition of the cyclised product [8–10]. The major volatile products from the first stage, identified by Tingfa and Deyuan [8,9] are 1,3-butadiene, cyclopentene, cyclohexadiene, vinyl cyclohexane, etc. The main reactions in the second stage are dehydrogenation and decomposition of the residue formed in the first stage. The DSC [8–10] analysis of HTPB in N_2 atmosphere has indicated the first stage as exothermic and second stage as endothermic. The exothermicity is due to the energy released in the formation of new bonds during crosslinking and cyclisation of HTPB, which is greater than the absorbed energy for bond scission during depolymerisation.

Table 2 shows that while the temperature of reaction is not much affected by molecular weight, there is an increase in mass loss in the first stage decomposition as the molecular weight of the samples decreases. This can be due to increased cyclisation and crosslinking at the expense of depolymerisation in high molecular weight samples and hence decreased weight loss, whereas in the case of low molecular weight samples, after the completion of cyclisation

Table 2
Thermogravimetric data of samples

Mol. wt. (M_n)	First stage				Second stage			
	T_i (°C)	T_f (°C)	T_s (°C)	% wt. loss	T_i (°C)	T_f (°C)	T_s (°C)	% wt. loss
14980	320	414	406	7.6	416	510	474	90.3
5690	300	410	402	7.7	412	510	474	90.3
2550	300	414	396	10.8	416	510	478	88.2
2360	300	410	402	11.3	412	510	474	85.9
1260	300	410	392	12.0	412	510	474	84.9
660	300	409	388	18.1	412	510	472	79.7

Table 3
Kinetic parameters of the degradation of HTPB

Mol.wt. (M_n)	First stage			Second stage		
	E (kJ mol^{-1})	A (s^{-1})	r	E (kJ mol^{-1})	A (s^{-1})	r
Coats–Redfern Equation						
14980	171.9	1.41×10^{11}	0.9993	272.8	8.13×10^{16}	0.9997
5690	154.9	8.71×10^{9}	0.9998	262.7	2.04×10^{16}	0.9994
2360	143.0	8.91×10^{8}	0.9995	259.0	1.12×10^{16}	0.9993
1260	136.3	2.69×10^{8}	0.9990	261.0	1.55×10^{16}	0.9998
660	96.7	1.66×10^{5}	0.9990	257.6	1.02×10^{16}	0.9997
2550	131.5	9.77×10^{7}	0.9990	279.1	2.69×10^{17}	0.9998
MacCallum–Tanner Equation						
14980	175.1	2.88×10^{11}	0.9993	278.4	2.88×10^{17}	0.9996
5690	158.1	1.66×10^{10}	0.9997	268.2	7.07×10^{16}	0.9995
2360	146.1	1.66×10^{9}	0.9996	264.2	3.80×10^{16}	0.9994
1260	139.4	5.01×10^{8}	0.9991	266.4	5.25×10^{16}	0.9998
660	99.3	2.88×10^{5}	0.9990	263.0	3.39×10^{16}	0.9995
2550	134.6	1.78×10^{8}	0.9988	284.7	1.00×10^{18}	0.9997
Horowitz–Metzger Equation						
14980	196.1	1.23×10^{13}	0.9981	290.0	1.58×10^{18}	0.9992
5690	171.1	1.90×10^{11}	0.9995	283.2	6.02×10^{17}	0.9991
2360	168.0	9.33×10^{10}	0.9983	279.5	3.47×10^{17}	0.9990
1260	156.6	1.26×10^{10}	0.9970	282.6	5.50×10^{17}	0.9994
660	118.3	1.05×10^{8}	0.9999	279.6	3.89×10^{17}	0.9991
2550	152.9	5.37×10^{9}	0.9988	303.9	1.58×10^{19}	0.9996
Madhusudanan–Krishnan–Ninan Equation						
14980	172.1	1.58×10^{11}	0.9992	272.8	8.71×10^{16}	0.9996
5690	155.1	9.77×10^{9}	0.9996	262.8	2.19×10^{16}	0.9994
2360	143.2	1.00×10^{9}	0.9995	258.8	1.23×10^{16}	0.9994
1260	136.5	3.09×10^{8}	0.9990	261.0	1.66×10^{16}	0.9998
660	96.9	1.95×10^{5}	0.9990	257.6	1.09×10^{16}	0.9996
2550	131.7	1.09×10^{8}	0.9986	279.2	2.95×10^{17}	0.9997

and crosslinking, decomposition starts at an earlier stage. Similar observations were made by Tingfa [8].

3.3. Thermal degradation kinetics

For the first stage, the value of n was found to be 0.5 and for the second stage 1 for all the fractions and the original sample. By substituting the values of n in the four kinetic equations, E and A were calculated for all the samples. The values of E, A and the correlation coefficients (r) are given in Table 3. The Horowitz–Metzger method shows higher values of kinetic parameters than those obtained by the other three methods. This is due to the approximation technique used in the integration of the former method.

The correlation coefficients of all the 24 plots are close to 0.999, which show the linearity of the fit. From the table it can be seen that for the first stage decomposition, the effect of molecular weight on E and A is more prominent than for the second stage decomposition. Both E and A are found to increase with increase in molecular weight. This may be attributed to the formation of greater number of cyclised/crosslinked products formed in the first stage for molecules of higher dimensions. In contrast, for the second stage, the change in values of E and A is not as prominent as in the first stage. The kinetic para-

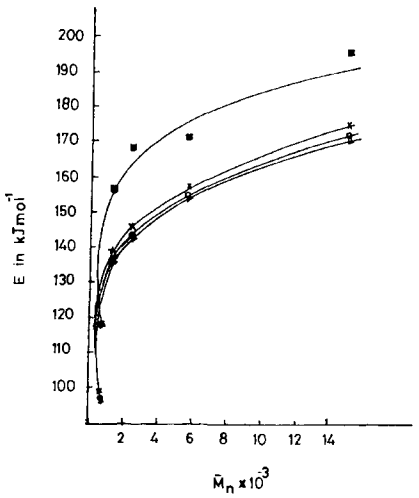

Fig. 3. Variation of activation energy (E) with M_n (△: CR, ○: MKN, ×: MT, and ■: HM).

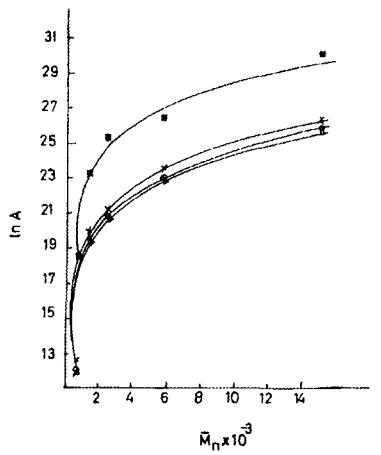

Fig. 4. Variation of pre-exponential factor (A) with M_n (△: CR, ○: MKN, ×: MT, and ■: HM).

meters for all fractions except the first one are nearly the same. This can be explained by the fact that the second stage is predominantly the decomposition of the cyclised and crosslinked products formed in the first stage. The differences in the size of molecular species produced diminishes after the crosslinking process taking place in the first stage. Therefore, the kinetic parameters of the second stage are not much affected by the molecular weight of the sample.

The regular trend in kinetic parameters relative to the GPC molecular weights of M_n, M_w and M_z for the first stage makes the data amenable for statistical treatment. It was found that for the first stage, E and $\ln A$ values from all four equations could be reasonably plotted against the molecular weights and Figs. 3 and 4 show the curves for M_n. Different types of curve fits were tried out with the data using a computer. It was found that the activation energy vs. different molecular weight (M_n, M_w, M_z) plots could be best represented by the following equations:

$$E = a_1 - a_2/M_n$$
$$E = b_1 - b_2/M_w$$

and

$$E = c_1 - c_2/M_z$$

where a_1, a_2, b_1, b_2, c_1 and c_2 are empirical constants for the different molecular weights. For pre-exponential factor (A) molecular weights were better correlated to $\ln A$. This can be explained on the basis of the kinetic compensation effect [20] postulating linear correlation between E and $\ln A$. The best fit curves were represented by the following equations:

$$\ln A = a_1' - a_2'/M_n$$
$$\ln A = b_1' - b_2'/M_w$$

Table 4
Curve fit constants from E vs. molecular weight plots

Equa tion	E vs. $1/M_n$			E vs. $1/M_w$			E vs. $1/M_z$		
	a_1	a_2	F	b_1	b_2	F	c_1	c_2	F
CR	168.4	4.68×10^4	70.0	170.0	7.51×10^4	45.5	171.9	1.18×10^5	16.1
MT	171.7	4.72×10^4	70.6	173.9	7.54×10^4	45.0	175.2	1.19×10^5	15.9
HM	189.8	4.64×10^4	70.7	192.9	7.50×10^4	30.9	193.4	1.18×10^5	13.8
MKN	168.6	4.68×10^4	70.0	170.9	7.51×10^4	44.9	172.1	1.18×10^5	16.4

Table 5
Curve fit constants from ln A vs. molecular weight plots

Equation	E vs. $1/M_n$			E vs. $1/M_w$			E vs. $1/M_z$		
	a'_1	a'_2	F	b'_1	b'_2	F	c'_1	c'_2	F
CR	25.2	8.59×10^3	81.8	25.6	1.38×10^4	46.8	25.8	2.15×10^4	15.8
MT	25.9	8.68×10^3	79.3	26.3	1.39×10^4	46.3	26.5	2.18×10^4	15.8
HM	28.8	6.95×10^3	31.9	29.1	1.13×10^4	33.0	29.4	1.18×10^4	18.3
MKN	25.3	8.56×10^3	79.8	25.7	1.37×10^4	46.2	29.9	2.15×10^4	15.7

and

$$\ln A = c'_1 - c'_2/M_z$$

where a'_1, a'_2, b'_1, b'_2, c'_1 and c'_2 are empirical constants for different molecular weights. The relation obtained for both E vs. molecular weights and ln A vs. molecular weights are same for all the kinetic equations (CR, MT, HM, MKN), but with different numerical values. The reliability of these curve fits was tested by the F-test [18]. The results of the empirical constants and F-values of the curves are given in Tables 4 and 5. For all the curves the calculated Fisher values are much higher than the critical F-values for 95% confidence level (10.1) indicating good reliability of the curve fits. In the case of M_n, all the values are higher than even the critical F-value for 99% confidence level (34.1). E or ln A vs. M_n is better, when compared to the M_w and M_z curves, probably due to the dependence of the first stage decomposition on the number of molecules present (from which M_n is calculated).

Acknowledgements

We thank the director of VSSC for the kind permission to publish this work. Thanks are due to Ms. K.B. Catherine for the GPC analysis, to Mr. G. Viswanathan Asari for help in TG analysis and Dr. K. Krishnan for helpful discussions. One of us, Sreelatha S. Panicker, thanks the Council of Scientific and Industrial Research, Government of India, for a Senior Research Fellowship.

References

[1] N.S. Cohen, R.W. Fleming and R.L. Deer, AIAA J. 12 (1974) 212.
[2] W. Zhong Yong and Ying Quan, Chem. Propellants 1 (1981) 12.
[3] A.M. Varney and W.C. Strahle, Combust. Flame 16 (1971) 1.
[4] W.H. Beck, Combust. Flame 70(2) (1987) 171.
[5] K.N. Ninan and K. Krishnan, J. Spacecraft and Rockets 19 (1982) 92.
[6] K.N. Ninan, K.B. Catherine and K. Krishnan, J. Thermal Analysis 36 (1990) 855.
[7] K.N. Ninan, K. Krishnan, R. Rajeev and G. Viswanathan, Thermoanalytical investigation of the effect of atmospheric oxygen on HTPB resin, Propellants, Explos. and Pyrotechnics, 21 (1996) 199.
[8] Du Tingfa, Thermochim. Acta 138 (1989) 189.
[9] D. Deyuan, Proc. 39th IAF Congress, Bangalore (1988).
[10] D. Tingfa and Liu Junfing, Thermochim. Acta 184(1) (1991) 81.
[11] W.S. Schnieder and R.W. Matton, Polym. Eng. Sci. 19 (1979) 1122.
[12] R. Nagappa and M.R. Kurup, AIAA Paper No. 90-2331 (1990).
[13] ASTM D-3593-80, Vol. 8.03, Annual Book of ASTM Standards by American Society for Testing and Materials (1989).
[14] A.W. Coats and J.P. Redfern, Nature 201 (1964) 68.
[15] J.R. MacCallum and J. Tanner, Eur. Polym. J. 6 (1970) 1033.
[16] H.H. Horowitz and G. Metzger, Anal. Chem. 35 (1963) 1464.
[17] P.M. Madhusudhanan, K. Krishnan and K.N. Ninan, Thermochim. Acta 97 (1986) 189.
[18] M. Mack, Essentials of statistics for scientists and technologists, Plenum press, New York (1976) pp. 106–115.
[19] M.A. Golub, J. Polym. Sci., Polym. Lett. 10 (1972) 41.
[20] P.D. Garn, J. Therm. Anal. 10 (1976) 99.